

## Tribological Characterization of Cocoa Mass with Different Rheological Properties and Particle Size Distributions

Florian Rummel<sup>1</sup>, Martina Tietz<sup>2</sup> and Shona Marsh<sup>3</sup>

<sup>1</sup>NETZSCH-Gerätebau GmbH, D-95100 Selb, Germany

<sup>2</sup>NETZSCH-Feinmahltechnik GmbH, D-95100 Selb, Germany

<sup>3</sup>NETZSCH-Gerätebau GmbH, Wolverhampton, United Kingdom

### ABSTRACT

Finely ground cocoa mass with varying particle size distributions were investigated using model scale tribology. The shear viscosity of molten cocoa mass influences the frictional behavior of a soft glass-elastomer tribocontact in the hydrodynamic friction regime. During the transition from static to dynamic friction, within the mixed and boundary friction regime, the behavior of the tribosystem cannot be explained by the differences in shear viscosity only. This paper discusses the interrelationship between the rheological properties of the cocoa mass sample and introduces possible mechanisms to explain the observed tribological behavior.

### INTRODUCTION TO FOOD TRIBOLOGY

Understanding the interrelationship between food structure and sensory perception of food is of particular interest in food science. Rheology has been, and still is, one of the most meaningful approaches in characterization of food materials. Food tribology has become a sought-after approach in this field, enabling the investigation of food oral processing<sup>1</sup>. During a tribological study, the behavior of an entire system – the tribosystem – is of interest. In food oral processing, tribosystems are representative of food intake, mastication and swallowing, with the tongue-palate tribopair lubricated by a food-saliva mixture. One major motivation is to gain insights into the mouthfeel of food by tribological studies using model system testing of food. Since the tribological behavior of a lubricated tribosystem is influenced by the rheological properties of the lubricant, rheological and tribological characterization often go hand in hand, enabling a deepened understanding of the food material and how it behaves as part of a tribosystem<sup>2</sup>.

The tribology of food suspensions and confectionery products in particular has been studied in recent years<sup>3-8</sup>. Different types of instrumentation are implemented in this field and using rheometers for tribological studies is one possible approach<sup>9</sup>. However, the concept of extended Stribeck curves has rarely been applied to such food materials<sup>10</sup>.

This research presents a complementary approach including rheological characterization of cocoa mass as a food sample and how this behaves at soft and low pressure tribocontacts.

## **MATERIALS AND METHODS**

### **Cocoa mass preparation**

Cocoa mass samples with approximately 56% fat content (measured with near infrared spectroscopy) were prepared from one batch of cocoa mass. This ensures that the composition of the cocoa mass sample is the same for both rheological and tribological characterization. The cocoa mass was finely ground on a horizontal ball mill (NETZSCH-Feinmahltechnik GmbH, Germany).

### **Particle characterization**

For light-microscopy analysis of the cocoa mass particles, 2 ml of the molten cocoa mass was dispersed in 50 ml of acetone in conical plastic tubes using a Pasteur pipette. The dispersion was left for approximately 12 hours for the particles to sediment. After this sedimentation period, the remaining acetone was removed from the conical plastic tube using a Pasteur pipette. This procedure was undertaken three times in order to sufficiently reduce the fat surrounding the particles. The acetone was left to evaporate at room temperature after the third sedimentation was complete. Microscopic analysis was undertaken on a Keyence VHX reflected light microscope equipped with a VH-Z500R objective and 500x magnification (Keyence, Japan). A minimal amount of cocoa mass particles applied via a spatula tip was placed on the microscope slides in addition to ~2 ml of acetone in order to separate the particles. The acetone evaporated immediately and the microscopy images were observed in a dry state.

Particle size distribution measurements were performed on a Mastersizer 3000 laser diffraction particle size instrument equipped with a manual wet dispersion unit (Malvern Panalytical, Malvern, United Kingdom). The cocoa mass sample was taken from a heating cabinet with a temperature of 50°C. After stirring the sample with a dry spatula ensuring a homogenous sample, 2 g of cocoa mass was dispersed in 50 g of a synthetic mineral oil (OKS Oil). Using a clean spatula, the sample was stirred and subsequently placed into an ultrasonic homogenizer for two minutes at an intensity of 33% to dissolve all agglomerates. The wet dispersion unit was operated with the synthetic mineral oil (OKS Oil). For each measurement, a small volume of cocoa mass sample (16-18%) was added with a Pasteur pipette to the dispersion unit. The Fraunhofer scattering model which assumes that all particles are round and opaque and which can be applied for cocoa particles<sup>11</sup> was used in this study. The particle size distribution measurements were carried out in double determination.

### **Rheological measurements**

Rheological measurements were carried out on a Kinexus Prime ultra+ rotational rheometer equipped with a Peltier-cylinder cartridge (NETZSCH-Gerätebau GmbH, Germany). A C14 concentric cylinder measuring geometry was used, consisting of a stainless steel cup coupled with an Aluminum bob and passive hood, suitable for a relatively low sample volume. The C14 measuring gap of 0.7 mm is suitable for characterization of the cocoa mass samples used in this study. The instrument was set to 40°C, approximately 1 hour prior to the measurement, in order to heat up the measuring geometry homogeneously. The zero gap was determined prior to each rheological measurement.

The molten cocoa mass sample was directly transferred from a heating cabinet FED53 (Binder, Tuttlingen, Germany) set to 40°C. The cocoa mass sample was contained in a 150 ml plastic beaker with lid. The lid was removed shortly before the measurement and the respective cocoa

mass sample was stirred thoroughly with a dry spatula for approximately 30 seconds to ensure a homogenous sample. This is of particular importance due to the tendency of solid cocoa particles to sediment. Approximately 3 ml of sample was transferred to the rheometer using a Pasteur pipette. The tips of the Pasteur pipettes were cut to increase their diameter from approximately 1.5 mm to approximately 3 mm. This was to reduce the risk of phase separation and particle agglomeration in the pipette.

After lowering the upper measuring geometry to the measuring position, the sample was pre-sheared for 2 min at a constant shear rate of  $5 \text{ s}^{-1}$  enabling sample homogenization and a defined sample history. Pre-shearing was followed by a 5 min waiting phase during which the shear stress was set to 0 Pa. A logarithmic viscometry shear rate table, starting from  $1 \text{ s}^{-1}$  up to  $50 \text{ s}^{-1}$  capturing 11 samples per decade was carried out. Immediately afterwards, the shear rate was lowered from  $50 \text{ s}^{-1}$  to  $1 \text{ s}^{-1}$ . Measurement points were recorded when the sample reached equilibrium. This procedure was repeated three times using a new sample for each measurement. Between the measurements, the measuring geometries were cleaned with dry paper tissues in order to avoid any contact with water since even small quantities of water affect the physical properties of confectionery masses<sup>12</sup>.

### Tribological measurements

Tribological measurements were undertaken on a Kinexus Prime ultra+ rotational rheometer equipped with a Peltier-plate cartridge with active hood and a ball-on-three-pins tribology cell (NETZSCH-Gerätebau GmbH, Germany). The upper measuring geometry included a borosilicate glass ball measuring 12.7 mm in diameter and SIL 30 silicone urethane elastomer (Carbon Inc., USA) pins were used as lower specimen representing the soft oral tongue-palate tribopair. The ball is pressed against the pins and the distance between the rotational axis and the ball-pin contact is  $R$ . The pins are inclined at  $45^\circ$  relative to the horizontal. The shaft rotates with a defined angular velocity that corresponds to the respective sliding speed at the tribocontact (see Fig. 1 on the left). The torque required for this rotational movement is recorded during the tribological measurement.

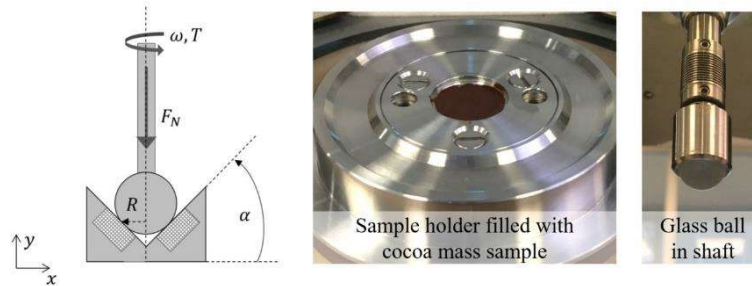


**FIGURE 1:** Schematic of the measuring geometry and the tribocontact (left) and sample holder with cocoa mass sample (middle) and upper geometry with glass ball (right)

The frictional force is calculated from the torque and the effective radius of the contact point of the ball on the pins  $R$

$$F_F = \frac{T}{R} \quad (1)$$

The normal force at the tribocontact is  $F_L$  and the total normal force applied by the measuring geometry shaft  $F_N$  where the following interrelationship applies:

$$F_L = \sqrt{2} \cdot F_N \quad (2)$$

*S. Marsh et al.*

The coefficient of friction  $\mu$  is calculated from the frictional force  $F_F$  and the normal force  $F_L$  at the tribocontact  $F_L$ .

$$\mu = \frac{F_F}{F_L} \quad (3)$$

The sliding speed is calculated from the effective radius of the contact point of the ball on the pins  $R$  and the angular velocity  $\omega$

$$v_s = \omega \cdot R \quad (4)$$

The specimen ball and pins were cleaned with acetone and paper tissues before placing them in the upper measuring geometry shaft or in the lower sample holder respectively. The glass ball was kept in the measuring geometry shaft during this study and was cleaned using dry paper tissues between measurements. This was required to avoid any contact with water. New pins were used for every measurement. The instrument was set to 40°C approximately 1 hour prior to starting the measurements in order to heat the sample holder homogeneously. The zero gap was determined before the first measurement. A normal force of 1 N was applied during the measurement. Using relatively soft specimen results in low contact pressures that simulate the soft contacts that occur during oral processing of food. The measurements were performed at 40°C which is close to body temperature and the common test temperature in confectionery rheology at which the cocoa butter is molten.

Prior to each measurement, the molten cocoa mass sample was transferred using a Pasteur pipette with an increased diameter as previously described. The sample volume was approximately 0.5 ml in order to make sure that all pins were fully covered with sample (see **Fig. 1** in the middle) when the glass ball (see **Fig. 1** on the right) is pressed against the pins. After loading the sample, a normal force of 1 N is applied for 2 min.

The normal force of 1 N is kept constant throughout the entire measurement. A 10 min running-in of the tribosystem was conducted at 15 rad·s<sup>-1</sup>. Subsequently to running-in, a holding phase of 5 min was performed in order to provide the tribosystem time to relax from the exposed stress. After the holding phase, the angular velocity is increased logarithmically from 5·10<sup>-6</sup> rad·s<sup>-1</sup> to 100 rad·s<sup>-1</sup> with 15 measuring points per decade. This refers to a sliding speed of 2.25·10<sup>-8</sup> m·s<sup>-1</sup> and 4.5·10<sup>-1</sup> m·s<sup>-1</sup>, respectively. This part of the measurement sequence is referred to as an extended Stribeck curve measurement<sup>13</sup>. Directly after the maximum angular velocity of 100 rad·s<sup>-1</sup> was reached, it was lowered to 5·10<sup>-6</sup> rad·s<sup>-1</sup>. This part of the measurement sequence is referred to as a Stribeck curve measurement. The procedure of increasing and decreasing the speed was repeated twice during each measurement, each repetition is called a run.

## RESULTS AND DISCUSSION

### Particles and particle size distributions

An example microscopy image of the cocoa particles within the cocoa mass medium is shown in **Fig. 2**. Particles with different size, color and shape can be observed in the sample. Results from the particle size distribution measurements are shown in the form of volume density distributions. The arithmetic mean of two measurement repetitions and the d<sub>90</sub> volume equivalent diameter is 33 μm for the coarse cocoa mass sample, 26 μm for the medium cocoa mass sample and 20 μm for the fine cocoa mass sample.



**FIGURE 2:** Light microscopy picture of cocoa mass particles

### Viscosity results and model fitting

Results from the rheological measurements are shown in the form of viscosity flow curves. **Fig. 3** shows the viscosity flow curves at increasing shear rates for all three samples. The points in the diagram represent arithmetic mean values from triple determination, with error bars indicating standard deviation. The discrete data points are connected by dotted lines for better visualization.

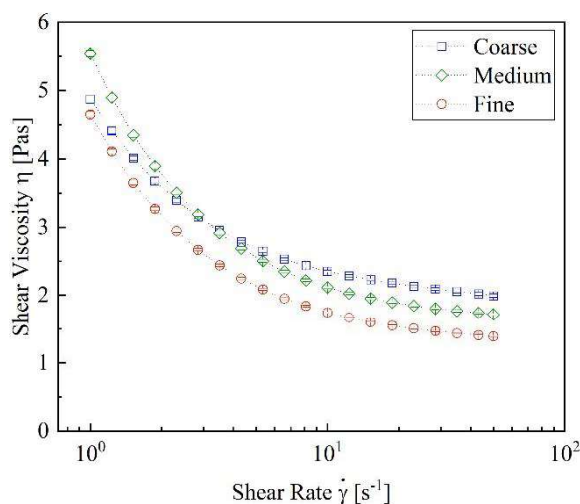


**FIGURE 3:** Viscosity curves of cocoa mass samples with different particles size distributions.

It can be seen that at higher shear rates ( $\dot{\gamma} > 3 \text{ s}^{-1}$ ), the shear viscosity is highest for the coarse cocoa mass sample and lowest for the fine cocoa mass. At lower shear rates ( $\dot{\gamma} < 3 \text{ s}^{-1}$ ), the shear viscosity of the medium cocoa mass sample is higher than the shear viscosity of the coarse cocoa mass sample. The decreasing shear viscosity at higher shear rates can be explained by the release of free fat during grinding. This yields lower volume of liquid effectively bound to the particles, and hence, a higher volume of liquid present, encouraging flow and subsequently decreasing viscosity<sup>14</sup>.

Viscosity flow curve measurements were fitted to the Herschel-Bulkley model which is considered a suitable model for chocolate samples<sup>15,16</sup>, therefore selected due to the structural similarity between cocoa mass and chocolate.

$$\tau = \tau_0 + K\dot{\gamma}^n \quad (5)$$

Here,  $\tau$  represents the shear stress,  $\tau_0$  the yield stress,  $K$  the consistency index,  $\dot{\gamma}$  the shear rate and  $n$  the flow behavior index. As one can expect for concentrated coarse suspensions, the flow index  $n$  in the Herschel-Bulkley model is  $< 1$ , indicating shear-thinning behavior of the samples (see **Table 1**). The fitted yield stress is lowest for the coarse particle cocoa mass and highest for the medium cocoa mass. The increase in the fitted yield stress from coarse to medium cocoa

mass can be explained by an increase in particle-particle interaction<sup>17</sup>. The decrease in the fitted yield stress comparing the medium and the fine cocoa mass cannot simply be explained by the change in particle size. As for the decrease in  $K$ , the possible increase of free fat may explain why the fitted yield stress decreases with further particle size reduction. This remains an assumption and requires further measurements of the free fat in the cocoa mass.

**TABLE 1:** Herschel-Bulkley fit parameters

Sample	$\tau_0$ [Pa]	$K$ [Pa s <sup>n</sup> ]	$n$
Coarse	2.55	2.36	0.951
Medium	3.88	1.85	0.969
Fine	3.30	1.55	0.960

### Stribeck curves and extended Stribeck curves

Results from the second measurements are shown in the form of Stribeck curves and extended Stribeck curves (see **Fig. 4**). The points in the diagrams represent arithmetic mean values from triple determination with error bars indicating standard deviation. The discrete data points are connected by dotted lines for better visualization.

The Stribeck curves and extended Stribeck curves, indicate that friction in the hydrodynamic regime is highest for the coarse cocoa mass sample and lowest for the fine cocoa mass sample. The transition from the mixed friction regime to the hydrodynamic regime occurs at lower sliding speeds when the coarse cocoa mass sample is measured, and at highest sliding speeds when measuring the low cocoa mass sample. This result is to be expected due to the shear viscosities of the samples at higher shear rates.

In both the mixed friction regime and the transition from the mixed friction regime to boundary friction, an inversed result in the friction is observed. This cannot be explained by the shear viscosities of the samples. A local maximum in friction for the fine cocoa mass sample can be seen, whereas for the coarse cocoa mass sample, this is not the case.

In the Stribeck curves, with further decreasing sliding speeds there is no clear difference visible between the three samples.

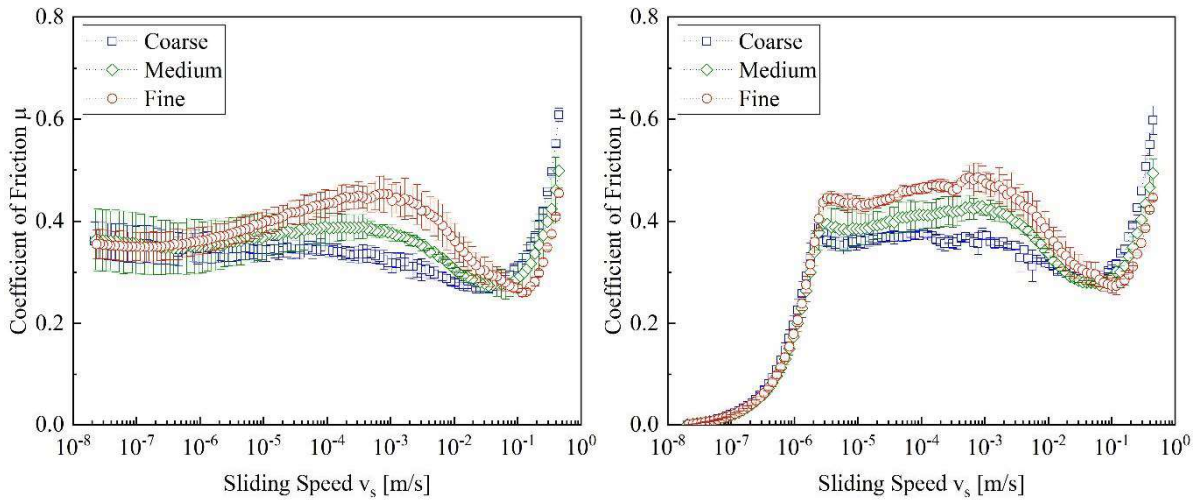


**FIGURE 4:** Stribeck curves (left) and extended Stribeck curves (right) for the tested cocoa mass samples with different particle size distributions

The increase in friction at the lowest sliding speed in the extended Stribeck curve measurement is due to deformation of the soft specimen. The curves for all three samples overlap, indicating that this behavior is predominately due to the bulk properties of the soft specimen.

The limiting friction is highest for the fine cocoa mass sample. For the coarse cocoa mass sample it is lowest. For the medium cocoa mass sample, there is no difference visible in limiting friction compared to the coarse cocoa mass sample. For the coarse cocoa mass sample, a distinct drop in the friction can be seen once the limiting friction has been overcome.

The lubrication mechanisms shown in **Fig. 5** are possible explanations for the observed frictional behavior that cannot be explained by differences in the shear viscosity of the cocoa mass.

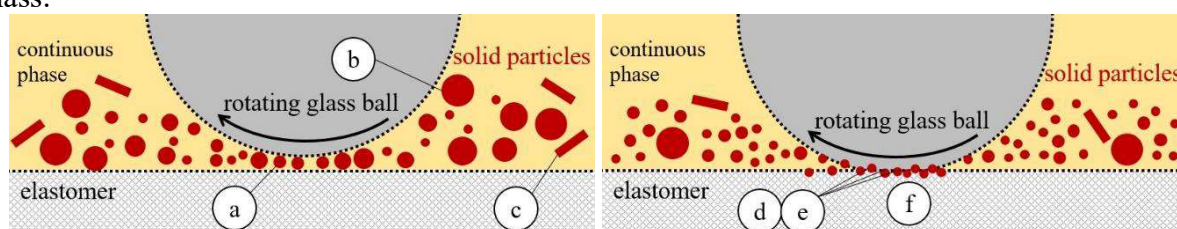


**FIGURE 5:** Schematics of possible lubrication mechanism for coarse particles (left) and smaller particles (right)

Coarse particles act as rollers (a) yielding lower friction<sup>18</sup>. This can be a possible explanation to the drop in friction after exceeding the limiting friction. Coarse particles are too big to enter the tribocontact (b), and hence lower viscosity of the sample at the tribocontact (lowered solid volume fraction) yields lower friction. Coarse and non-spherical particles are sterically hindered from entering the tribocontact (c) and therefore lower viscosity of the sample at the tribocontact (lowered solid volume fraction) yields lower friction.

Small particles sticking to the soft specimen surfaces (d) effectively increase surface roughness. The embedding of particles to soft surfaces has already been proposed by Lee et al.<sup>3</sup>. Higher numbers of small particles cause high numbers of interactions and interlocking of particles (e) consequently increasing friction. Small particles do not separate the specimen surfaces effectively (f) and hence, increased surface area results in higher friction.

## CONCLUSION AND OUTLOOK

In order to understand the lubricating mechanism in the mixed and boundary friction regime, further studies are required. Such studies may include testing of simplified model systems with defined particle size and shape.

To assist and gain insight into food manufacturing, the interrelationship between frictional behavior and the sensory perception of food could be studied. Such studies are not limited to cocoa mass, and may include more complex confectionery products such as filling masses or chocolate. Here, the role of saliva or artificial saliva may also be an influencing factor<sup>6,19</sup>.

Furthermore, tribological approaches in food processing are not just relevant with regard to mouthfeel, they are also applicable in operations such as pumping or grinding. The interaction between the product (such as cocoa mass in this research) and the equipment, can be investigated, e.g. to study wear mechanisms of components such as pump stators, rotors or grinding media.

Considering food structure from a sensory perception point of view but also from the perspective of process engineering, may serve as key to optimizing processes from a global perspective. This includes machinery and process parameters being optimized to manufacture ideal food that matches consumers' high expectations but also design and operate conditions in a more sustainable procedure through wear reduction or energy-saving processing.

## **Bibliography**

1. In order Chen J. and Stokes J.R., Rheology and tribology: Two distinctive regimes of food texture sensation, *Food Science and Technology*, **2012**, 25 (1), 4-12. DOI: 10.1016/j.tifs.2011.11.006.
2. Stokes J.R, Boehm M.W., and Baier S.K., Oral processing, texture and mouthfeel: from rheology to tribology and beyond, *Current Opinion in Colloid & Interface Science*, **2013**, 18 (4), 349-359. DOI: 10.1016/j.cocis.2013.04.010.
3. Lee S., Heubeger M. Rousset P. et al. , A tribological model for chocolate in the mouth: General implications for slurry-lubricated hard/soft sliding counterfaces, *Tribology Letters*, **2004**, 16 (3), 239-249. DOI: 10.1023/B:TRIL.0000009735.06341.32.
4. Lee S., Biresaw G., Kinney M.P. et al., Effect of cocoa butter replacement with a  $\beta$ -glucan-rich hydrocolloid (C-trim30) on the rheological and tribological properties of chocolates, *Journal of the Science of Food and Agriculture*, **2008**, 89 (1), 163-16. DOI: 10.1002/jsfa.3424.
5. Masen M. and Cann P.M.E., Friction measurements with molten chocolate, *Tribology Letters*, **2018**, 66 (1), 1-13. DOI: 10.1007/s11249-017-0958-x.
6. Samaras G., Bikos D., Vieira J., et al., Measurement of molten chocolate friction under simulated tongue-palate kinematics: effect of cocoa solids content and aeration, *Current Research in Food Science*, **2020**, 3 (1), 304-313. DOI: 10.1016/j.crfs.2020.10.002.
7. Zhu Y., Bhandari B., Prakash S., Relating the tribo-rheological properties of chocolate flavoured milk to temporal aspects of textures, *International Dairy Journal*, **2020**, 110 (1), 1-10. DOI: 10.1016/j.idairyj.2020.104794.
8. Schädle C.N., Sanahuja S., Bader-Mittermaier S., Influence of fat replacers on the rheological, tribological and aroma release properties of reduced-fat emulsions, *Foods*, **2022**.
9. Sarkar A. and Krop E.M, Marrying oral tribology to sensory perception: a systematic review, *Current Opinion in Food Science*, **2019**, 11 (6), 1-21. DOI: 10.3390/foods11060820.
10. Rummel F., Pondicherry K., Läger J. et al., Biotribological investigation as a key to food oral processing, Nordtrib conference poster presentation, **2018**.
11. Gould J., Vieira, J., Wolf, B., Cocoa particles for food emulsion stabilisation, *Food & Function*, **2013**, 4 (1), 1369-1375. DOI: 10.1039/c3fo30181h.
12. Beckett, S.T., *The Science of Chocolate*, The Royal Society of Chemistry, Cambridge, **2008**.
13. Pondicherry K., Rummel F., Läger J., Extended Stribeck curves for food samples, *Biosurface and Biotribology*, **2018**, 4 (1), 34-37. DOI: 10.1049/bsbt.2018.000.
14. Windhab E.J., Fluid Immobilization – a structure-related key mechanism for the viscous flow behavior of concentrated suspension systems, *Applied Rheology*, **2002**, 10 (3), 123-144. DOI: 10.1515/arh-2000-0009.
15. Sokmen A. and Gunes G., Influence of some bulk sweeteners on rheological properties of chocolate, *LWT Food Science and Technology*, **2006**, 39 (10), 1053-1058. DOI: 10.1016/j.lwt.2006.03.002.
16. Shah A.B., Jones G.P. and Vasikjevic T., Sucrose-free chocolate sweetened with Stevia rebaudiana extract and containing different bulking agents – effects on physicochemical and sensory properties, *International Journal of Food Science and Technology*, **2010**, 45 (1), 1426-1435. DOI: 10.1111/j.1365-2621.2010.02283.x.
17. Afoakwa E.O., Paterson A. and Fowler M., Effect of particle size distribution and composition on rheological properties of dark chocolate, *European Food Research and Technology*, **2008**, 226 (1), 1259-1268. DOI: 10.1007/s00217-007-0652-6.
18. Rudge R.E.D., van den Sande, J.P.M., Dijkman J.A. et al., Uncovering friction dynamics using hydrogel particles as soft ball bearings, *Soft Matter*, **2020**, 16 (1), 3821-3831, DOI: 10.1039/D0SM00080A.
19. Laguna L., Fiszman S., Tarrega A., Saliva matters: Reviewing the role of saliva in the rheology and tribology of liquid and semisolid foods. Relation to in-mouth perception, *Food Hydrocolloids*, **2021**, 116 (1), 1-11. DOI: 10.1016/j.foodhyd.2021.106660.